Experiment deduction efficiency of an electrostatic precipitator by online measurement of the surface potential pollution layer

Houari HASKAR[1], Farid MILOUA[1], Abbès OUARI[1], Amar TILMATINE[1]

[1]Applications of Plasma, Electrostatics and Electromagnetic Compatibility Research Unit APELEC, University Djillali Liabès of Sidi Bel-Abbès, Algeria

E-mail : milouafarid@gmail.com

***Abstract* -** Electrostatic precipitators (ESPs) are the most prevalent devices used for separating dust, fumes, or fog from gas. Numerous factors are involved in a filtration process, which requires the optimization and continuous monitoring of collection efficiency. Resistivity is one of the crucial factors that significantly affect ESP performance. Resistivity has a particular effect on the performance of a dust layer deposited on a collecting electrode. Particles (e.g., PVC) that exhibit high resistivity are difficult to charge; however, they do not easily give up their acquired charge in contact with the ground electrode, which causes an increase in surface potential and consequently back corona phenomenon. Therefore, to achieve the optimal filtration efficiency, the electric field intensity must be maximum (close to the breaking voltage) for ensuring an improved loading of the particles having high resistivity, without forming an electric arc. This study proposed a new practical technique for controlling a wire-cylinder configuration ESP based on the automatic variation of high voltage by using a motorized potentiometer (PM) to maintain set-point discharge current. Automatic voltage control varies the power of a high- voltage power supply in response to signals received from the ESP. The surface potential of a pollution layer and its equivalent resistivity can be deduced in-situ under electrical discharge for different particle sizes.

***Keywords* -** Back corona; Control; Electrostatic precipitator; measurement; Sparks; Surface potential.

I. INTRODUCTION

Electrostatic precipitation is used to eliminate solid pollutants, (e.g., dust and ashes) or liquids (e.g., oil mist) contained in the gas injected into our environment. No filtering process is as effective as an electrostatic process [1]. The scope of this process currently extends to viable places (e.g., apartments, offices, and hospitals) and workshops (e.g., machine rooms) because of low electrical energy consumption and high filtration efficiency (up to 99.9%) [2]. Although it has high efficiency, ESP performance is always considerably influenced by physical parameters related to gas and dust [3, 4]. The resistivity of the dust layer deposited on electrodes is a very crucial feature for controlling precipitator performance [5, 6]. Resistivity is related to the physicochemical nature of dust. High resistivity causes back discharge [7, 8], which creates an arc between the two electrodes. This change in a discharge regime (from a diffuse corona discharge regime to an arc regime) significantly reduces collection efficiency [9]. Therefore, the resistivity of the particles or a porous layer of particles is a crucial parameter for the selection of operating voltage and reference current. Resistivity between 10^{+2} and 5.10+8 Ω.cm allows the normal functioning of the ESP [10]. PVC particles with known resistivity (greater than 10^{+8} Ω.cm) are selected, which allows the abnormal functioning of the filter, thus extensively using an online control and command system. An automatic voltage control command is adapted in this paper by using an Arduino card, which allows the variation of the power supply voltage, and thus, sparks in the ESP are timely extinguished [11, 12].

In addition to the control system, this paper aimed to study the experimental feasibility by which to calculate the resistance of the PVC powder layer accumulated over time on the collector electrode surface of the ESP. Equivalent resistance and its surface potential can be deduced using the in-situ measurement of discharge current, which must be varied around to the set-point current.

II. MATERIALS AND METHODS

A) Experimental Device

The realized test bench (Fig. 1) can be divided into three separate functional entities: the addition of PVC powder, filtration device, and command and control of the ESP. The admission of PVC powder (a majority size of 180 μm diameter) is provided by a vibro-transporter, which introduces the PVC powder directly into a funnel placed at the entrance of the ESP, with a fixed mass flow q_{int} = 0.5 g/s. The speed of powdery flow is controlled by a dust recovery cyclone ($Q_{Airflow}$ = 50 m^3/h), which allows the recovery of unfiltered powder. The filtration device is a conventional wire-cylinder ESP, having a length of 140 mm and diameter of 90 mm.

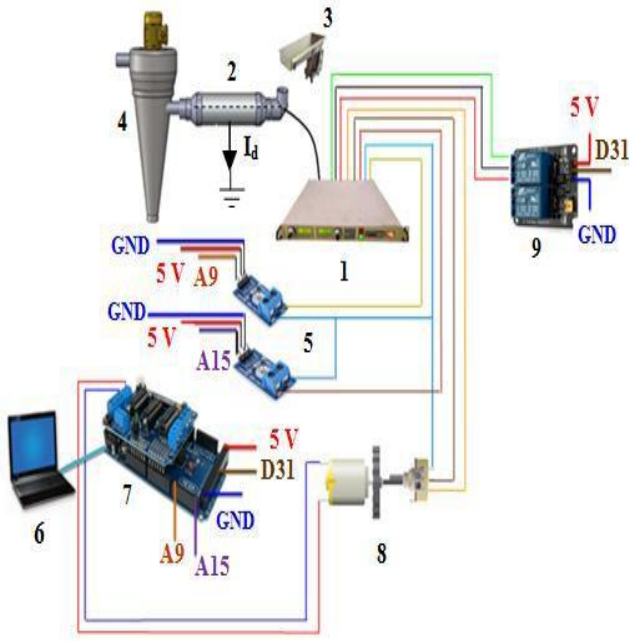

Fig. 1. Autopilot circuit of high-voltage power supply (Machine-Machine Interface).

1. Spellman high-voltage power supply, 2.ESP, 3.vibro-transporter, 4.recovery cyclone, 5. voltage sensors, 6. computer, 7. arduino + shield motor, 8. motorized potentiometer, and 9.relay module.

The corona wire with a diameter of 0.25mm is connected to a negative high-voltage supply (U_{max} = 40 kV, I_{max} = 7.5 mA, Model SL-300, Spellman). The control part of the filter primarily comprises an Arduino MEGA card, a motorized potentiometer, and voltage sensors.

The used HV generator (SPELLMAN SL-300) incorporated several features that allowed a progressive, manual increase in high voltage until the predefined operating point. In the local control (front panel control) of power supply, jumpers were installed on external interface TB1 (or J5) in the rear of the chassis between TB1–10 (J5–10) and TB1–11 (J5–11) for voltage control and between TB1–8 (J5–8) and TB1–9 (J5–9) for current control.

For automatic control, jumpers are eliminated, and a positive voltage source is applied to appropriate terminals. By adjusting the voltage source of the low-power circuit from 0 to 10 V, a voltage is varied for the high-power circuit (0–40 kV). Pins 5 and 6 on the back panel were used to monitor current and output voltage (Fig. 2).

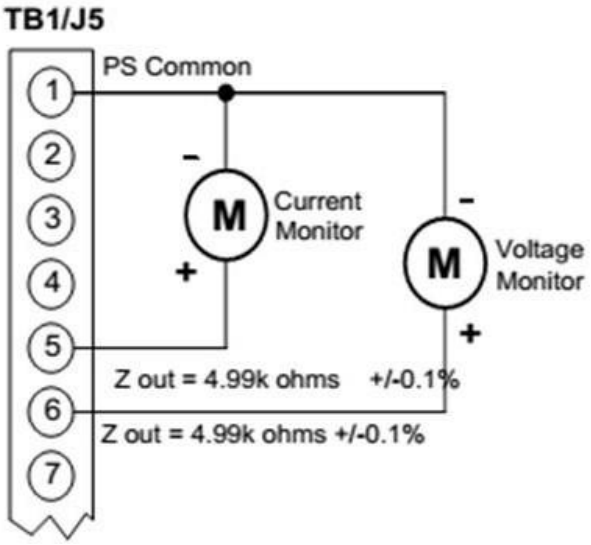

Fig. 2. Circuit for sampling current and voltage delivered by high-voltage generator.

Fig. 3 shows the circuit diagram, indicating that the following four distinct elements are connected to the Arduino card. Two voltage sensors, allowing data transfer (voltage and current), a relay module that opens or closes the power switch (ON and OFF) and automatically disables the high-voltage power supply in case of an arc, a motorized potentiometer for the automatic adjustment of the low-power circuit voltage of the power supply, and a shield module for controlling the potentiometer motor that generates a pulse width modulation (PWM) signal.

The Arduino (the central element) periodically collects measurements performed using voltage sensors. Discharge current delivered by the ESP is continuously compared with set-point current. If current exceeds, the Arduino card automatically reduces the supply voltage of the source through a motor shield to decrease potentiometer resistance.

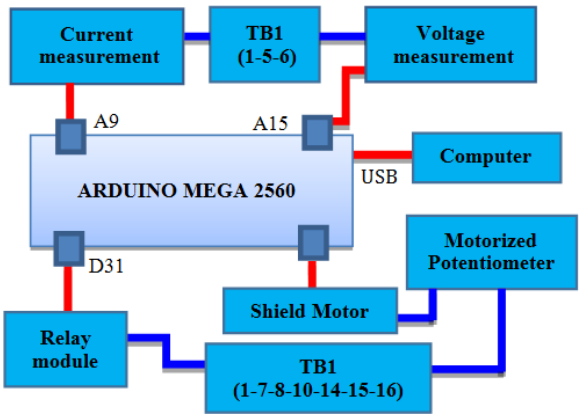

Fig. 3. Illustrative diagram of control circuit.

B) Determination of Set-point Current ($I_{set\text{-}point}$)

Before starting the ESP using its automatic control system, the limit of its normal operation must be known first without injection of PVC powder. The limit (For U = 32 kV) is obtained by manually varying the voltage at the highest level without causing excessive spark between the two electrodes.

In practice, the filtration is improved when the applied voltage is close to the breakdown voltage, in particular when the particles to be filtered have a high resistivity, similar to that of PVC [13, 14]. Fig. 4 indicates that the set-point current should not exceed 0.91 mA.

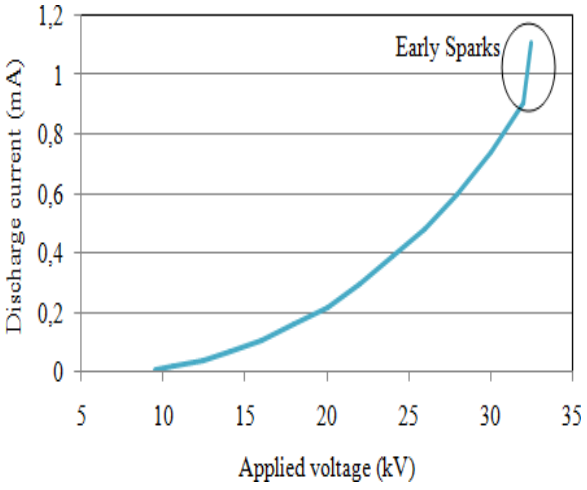

Fig. 4. Determination of operating limit point (U = 32 kV) of precipitator without powder.

C) Command Protocol

ESP control voltage is programmed after manually determining the set-point current. The Arduino MEGA and computer can interact through serial communications. The program (sketch) can be easily loaded by connecting the serial port of the Arduino to the computer. This process sends data from the computer to the Arduino, and the Arduino in turn sends status messages to the computer for confirming a successful transfer.

The commands sent from the Arduino card through the shield motor allow the motorized potentiometer to rotate in both directions at a required speed for $t_{forward}$ or $t_{backward}$ for regulating high voltage, thereby maintaining fixed discharge current. The aforementioned method is continuously compared on a sampling step ($t_{measure}$) with the consigned current. Fig. 5 shows the block diagram of principle outlining describing control protocol functionality

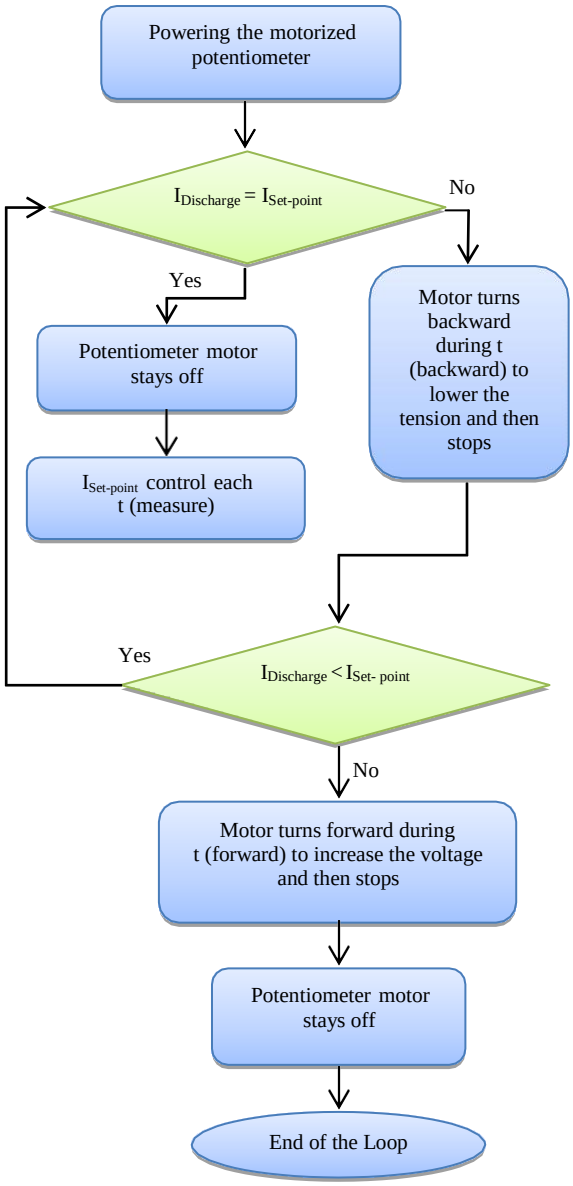

Fig. 5. Block diagram of voltage control and its operation

III. EXPERIMENTAL RESULTS AND DISCUSSION

An automatic voltage control technique allows the analog value of discharge current and applied voltage to be recorded using the function analogue Read. The potentiometer delivers an analog voltage between 0V (TB1-1) and 10V (maximum value of TB1-7).

Servo control in voltage must be performed numerically by comparing the applied current and the set-point current values for the shield motor to generate appropriate PWM signals that power the motorized potentiometer. The generation of PWM must consider the response time of the control system. Therefore, the rotation time of the potentiometer $t_{forward}$ and $t_{backward}$ must be controlled by the Arduino program to limit it within the maximum frequency of sparks.

A) Performance analysis of ESP

Efficiency of Filtration With or Without Voltage Control :

In this part of work, the expected goal is not to reach a yield close to 100 %, but to make a comparison between the efficiency obtained without and with automatic control. In fact, and in order to show the reliability of our technical control, we subjected the filter to the most unfavorable conditions (High suction flow, voltage applied to the breakdown limit)

Fig. 6 and Table 1 indicate the following:

- Filtration efficiency is approximately doubled for different operating times of the filter
- Significant reduction in the number of sparks

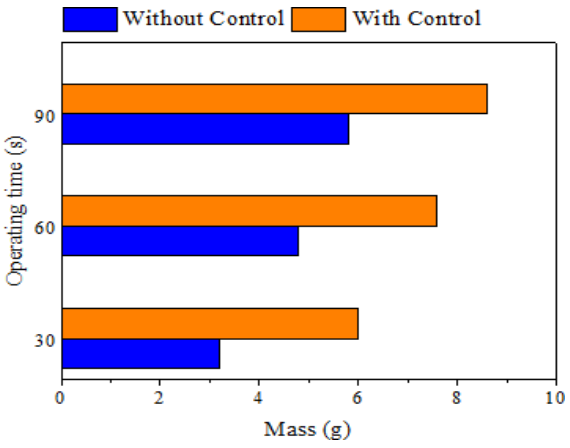

Fig. 6. Comparison of ESP performance with and without automatic control.

Table 1. Comparative results of filtration efficiency

Experiments	Time (s)	Collected mass (g)	Number of sparks	Efficiency (%)
Without control	30	3,2	20	21,33
	60	4,8	>20	16
	90	5,8	>30	12,89
Automatic control	30	6	1	40
	60	7,6	1	25,33
	90	8,6	1	19,11

Fig. 7 illustrates the online variation of discharge current after the automatic high-voltage control is triggered, with an ESP operating time of 210 s.

The control system response is approximately instantaneous because the nominal operating regime is realized. Current stabilizes when it reaches near the set-point current of 0.91 mA after passing through an unstable operating regime (very frequent presence of sparks).

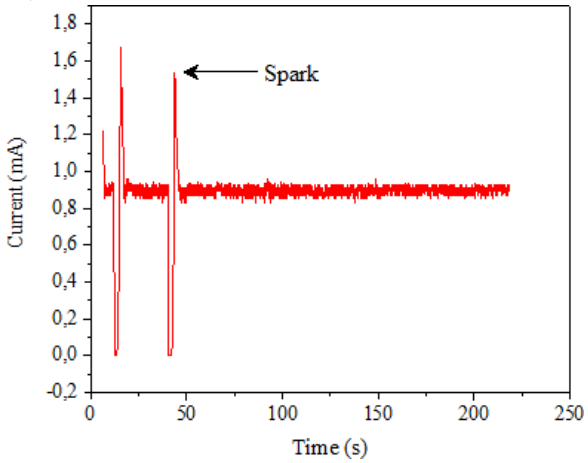

Fig. 7. Online variation of discharge current

During filtering, the collected dust layer behaves as an ascending variable resistance, thereby increasing its surface potential (V_{Sur}). Fig 8 represents surface potential measured in real time.

The regulation system reduces the applied voltage (Fig 9) because the PVC particles deposited on the collection electrode.

Therefore to maintain a discharge current near of the set-point current ($I_{Set\text{-}point}$ = 0.91 mA). The recorded voltage drop is proportional to PVC layer resistance because discharge current is maintained constant. It can be calculated using the following equation :

$$U_{App} - U_{Ins} = V_{Sur} = R_{PVC}(t).I_{set-point} \quad (1)$$

Where : U_{App} : Applied voltage (32 kV),

U_{Ins} : Instantaneous voltage applied (kV),

V_{Sur} : Surface potential (kV),

R_{PVC} (t): Equivalent resistance of the PVC layer as a function of time,

$I_{Set\text{-}point}$: Set-point current (0.91 mA).

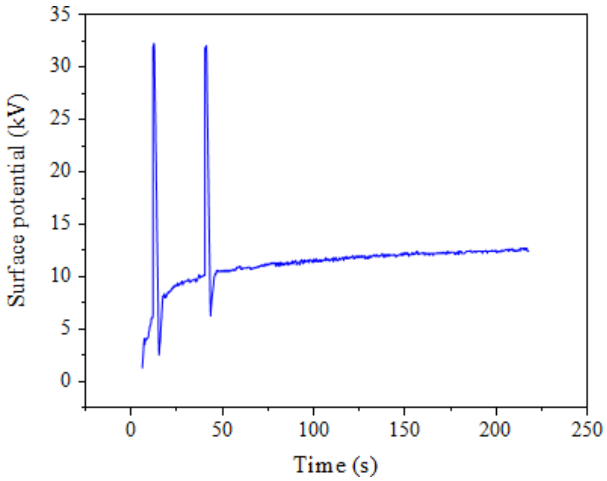

Fig. 8. Temporal variation of surface potential of PVC layer.

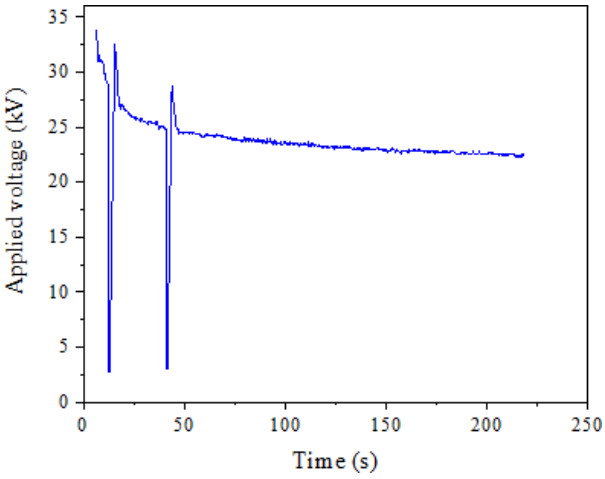

Fig. 9. Online regulation of applied voltage.

B) Influence of Particle Size on Surface Potential

Dust deposited on the collection electrode acts as a variable resistor in series with the ESP. Fig 10 indicates that surface potential is increasing regardless of the particle size. This is because the amount of collected material increases as a function of time, which increases its resistance.

Resistance of the PVC layer is inversely proportional to the particle size (Table 2). Moreover, the inter-particle distance decreases with the size decreases, which considerably reduces the dissipation of electric charges to the ground. Although the collected mass having a size of 90 µm is smaller than 125 µm and 180 µm, the value of the recorded resistance is considerably higher. This is due to the decrease in inter-particulate air volume which increases greatly the equivalent resistance value of the pollution layer.

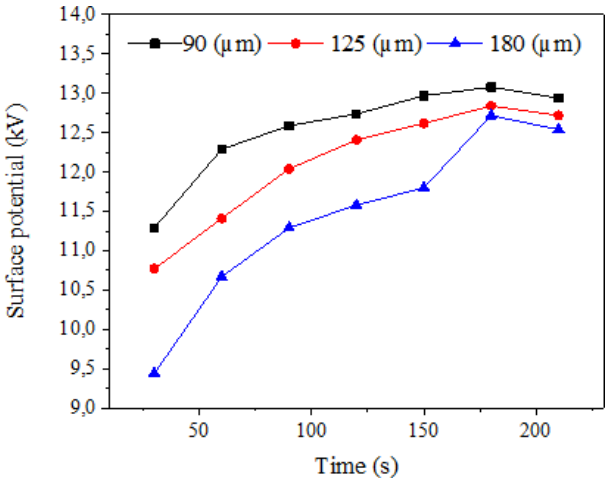

Fig. 10. Variation of surface potential according to size of PVC particles

Table 2. Relation between mass and equivalent resistance of collected dust layer.

Particles diameter (µm)	90		125		180	
Operating time (s)	M_c (g)	R (MΩ)	M_c (g)	R MΩ)	M_c (g)	R (MΩ)
30	3	12,66	4,1	12,016	6	10,57
60	4,4	13,5	5,5	12,75	7,6	11,88
90	5,3	14	6,5	13,54	8,6	12,62
120	6	14,45	7,3	14	9	12,95
150	6,6	14,8	7,7	14,2	9,6	13,45
180	7	15	8,2	14,54	10,3	14,19
210	6,2	14,67	7,5	14,29	10,1	14

C) Relationship Between Equivalent Resistance and Mass of Collected PVC Layer

To establish a relation between the resistance and mass of the collected PVC powder, mass measurements have been performed for different operating times of the ESP. The collected mass reaches its maximum value at 180s because of the saturation of the collection electrode and the excessive increase in the voltage drop.

From relation (1), the resistance value of the PVC layer can be calculated as follows :

$$R_{PVC}(t) = \frac{U_{App} - U_{Ins}}{I_{set-point}} \quad (2)$$

The variation in the mass and resistance of the PVC layer is plotted on the same figure (Fig 11) as a function of the ESP operating time. The two variations follow the same pattern, indicating that the resistance increases as a function of the mass of collected dust. This variation is quasi-linear (Fig 12).

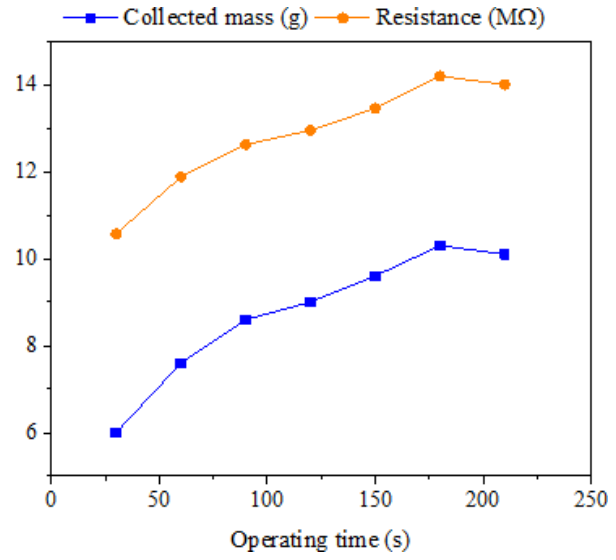

Fig. 11. Evolution of equivalent resistance and collected mass of PVC as a function of time

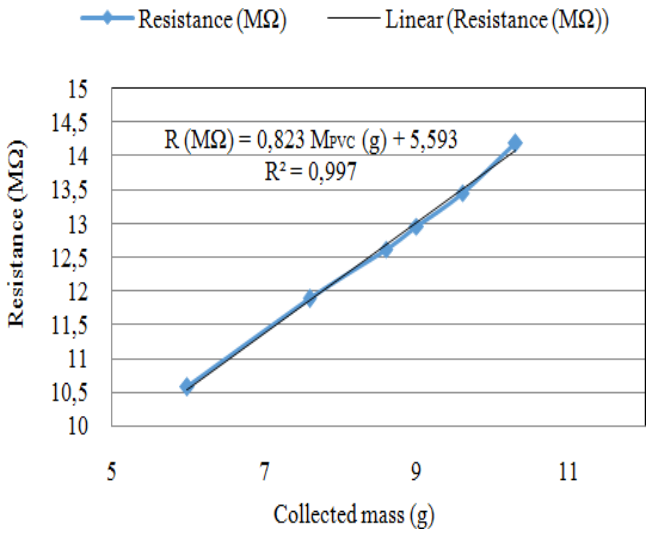

Fig. 12. Variation of PVC layer equivalent resistance as a function of collected mass.

D) Modeling of filtration process

1) Online Prediction of Filtration Efficiency

To anticipate filter performance as a function of time, the collected or outgoing mass must be known.

The variation of the collected mass as function of equivalent resistance is quasi-linear, thus efficiency can be expressed as a function of the PVC layer resistance. The prediction curve in Fig 13 indicates the efficiency as follows:

$$\mu(t) = \frac{M_{pvc}(R)}{t.q_{int}}.100 \quad (3)$$

$$\mu(t) = \frac{(1{,}21\,.R_{PVC}(t) - 6{,}743)}{t.q_{int}} \quad (4)$$

With: M_{pvc} (R): Mass collected as a function of the layer equivalent resistance (g),

q_{int}: Mass flow of PVC particles introduced in the ESP (0.5g/s),

R_{pvc} (t): Equivalent resistance of the PVC layer (equation 2), t: Filter operating time (s).

Efficiency variation as a function of time according to the relation (4) is represented using the following Fig 14:

The efficiency is maximum when the resistance value of the collected layer is maximum. For the experimental conditions, the rapping cycle must be less than 60s to ensure a yield of approximately 40%, which corresponds to the R_{PVC} resistance of less than 11.88 MΩ.

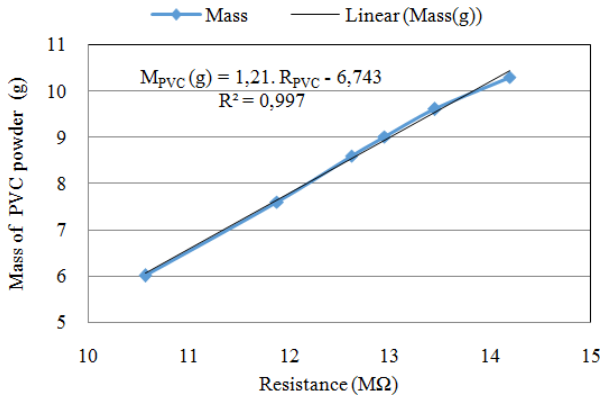

Fig. 13. Plot of variation of mass collected as a function of equivalent resistance

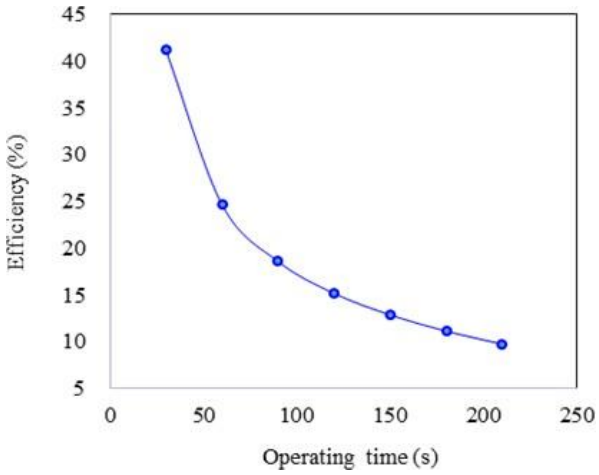

Fig. 14. Online variation of filtration efficiency.

2) In-situ Measurement of the Equivalent Resistivity of PVC Layer:

The in-situ principle is used for measuring the resistivity of the material during an electric discharge. However, the surface potential $V_{Sur}$of the material cannot be precisely determined. According to this method, the resistivity can be expressed as follows :

$$\rho_{PVC} = \frac{V_{Sur}}{e.J} \quad (5)$$

Where ρ_{PVC}, e, and J are electrical equivalent resistivity, the thickness of the dust layer, and the surface current density, respectively.

Another relation is available for determining the dust layer resistivity. The relation is obtained using the standard IEEE method for depositing a dust layer on a cell placed between the two parallel electrodes, and a voltage of a few kilovolts is then applied to the electrode system. Thus, the resistivity is calculated by measuring the current flowing through the dust layer. This relation given as follows :

$$\rho_{PVC} = \frac{S.U_{Ins}}{I_d.d} \quad (6)$$

Where S, d, and Id are the surface of the cylindrical collection electrode, inter-electrode distance, and instantaneous discharge current, respectively.

Fig. 15 shows an online sampling of equivalent resistivity (particle size =180 µm), each sampling having a duration $t_{measure}$ = 210s calculated using relation (6). The average value of resistivity is approximately $2.5.10^{+9}$ Ω.cm. Therefore, the frequency of sparks is high, without the voltage control system.

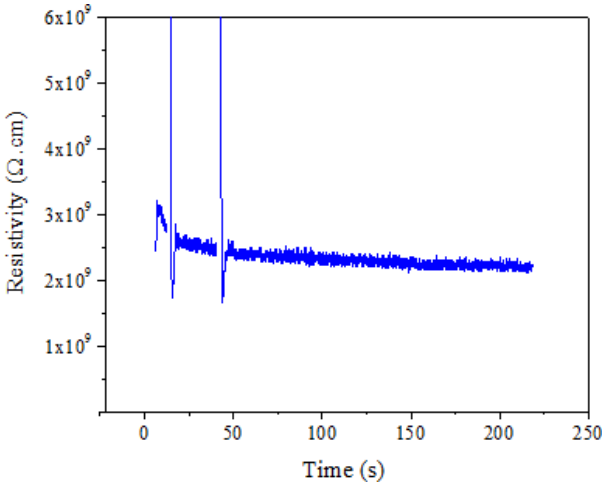

Fig. 15. Online deduction of the equivalent resistivity of PVC layer.

IV. CONCLUSION

This study was initially focused on controlling the ESP voltage by using a motorized potentiometer. This technique is very practical and has considerably reduced the frequency of sparks by using an automatic control for the discharge current produced by the ESP, which doubles collection efficiency from its original value. The in-situ deduction of the dust layer resistivity as a function of time can be performed when the value of the surface potential is known. The equivalent resistivity of the dust layer depends on several factors, such as particle size, compactness of the deposit, applied electric field strength, temperature, and humidity. Therefore, the instantaneous deduction of the pollution layer resistance provides an online evaluation of filtration efficiency.

V. REFERENCES

[1] F. Miloua, A. Tilmatine, S.M. Remaoun, D. Berrached, and M. Bengrit, "Application of electrostatic precipitator in collection of smoke particles from hospital wastes combustion,"International Journal of Environmental Studies vol. 70(4), pp. 527-535, 2013.

[2] S. Oglesby, and G. B. Nichols, "Electrostatic precipitation: Pollution Engineering and Technology,"Marcel Dekker Incorporated, 1978.

[3] T. Yamamoto, and Velkoff, H. R, "Electro hydrodynamics in an electrostatic precipitator," Journal of Fluid Mechanics, vol. 108, pp. 1- 18, 1981.

[4] J. Podlinski, A. Niewulis, J. Mizeraczyk, and P. Atten, "ESP performance for various dust densities," Journal of Electrostatics, vol. 66(5-6), pp. 246-253, 2008.

[5] H. T. Busby, and K.Darby, "Efficiency of electrostatic precipitators as affected by the properties and combustion of coal," J. Inst.Fuel, vol. 36 (5), pp. 184, 1963.

[6] J. Miller, B. Hoferer, and A. Schwab, A. J, "The impact of corona electrode configuration on electrostatic precipitator performance," Journal of Electrostatics, vol. 44(1-2), pp. 67-75, 1998.

[7] S. Masuda and A. Mizuno, "Flashover measurements of back discharge, "Journal of Electrostatics, vol. 5, pp. 215-231, 1978.

[8] C. Chesmond, and R. Truce, "Using electrostatic precipitators to collect highly resistive dust," Institute of Engineers Australia, Queensland Technical Papers, vol. 26 (9), pp. 16-20, 1985.

[9] H. J. White, "Resistivity problems in electrostatic precipitation,"Journal of the Air Pollution Control Association, vol. 24 (4), pp. 313-338, 1974.

[10] J. Zhu, Y. Shi, X. Zhang, H. Yan,, and K. Yan,"Current Density and Efficiency of a Novel Lab ESP for Fine Particles Collection," In Electrostatic Precipitation: 11th International Conference on Electrostatic Precipitation, Hangzhou, 2008(p. 65-69). Springer Science & Business Media, 2010.

[11] H. Wenge, and X.Haowang, "Non-static Collection Process of the electrostatic Precipitator," Electrostatic Precipitation, Springer link, pp. 79-83, 2009.

[12] K. Huang, "Spark and its effect on electrostatic precipitator," ICESP X, 10th International Conference on Electrostatic Precipitation, Cairns, Australia, 2006.

[13] P. Intra, P. Limueadphai, and N. Tippayawong, "Particulate emission reduction from biomass burning in small combustion systems with a multiple tubular electrostatic precipitator," Particulate Science and Technology, vol. 28(6): 547-565, 2010.

[14] Remaoun, S. M., F. Miloua, A. Tilmatine., N. Hammadi, N. Zouzou, and L. Dascalescu,"Optimization of a Cost-Effective Wire Plate-Type ESP for Installation in a Medical Waste Incinerator,". IEEE Transactions on Industry Applications, vol. 50 (2), pp. 1361-1396, 2014.